Journal of Al-Azhar University Engineering Sector

Vol.18, No. 69, October 2023, 830 - 849

EXPERIMENTAL INVESTIGATION ON THE DYNAMIC CHARACTERISTICS OF A SPAR-TYPE OFFSHORE WIND TURBINE UNDER IRREGULAR WAVES

Ahmed Youssef Kamal[1], A. M. Abou-Rayan[1], Amal Shalabe[1*], Mohamed Samy[2]

[1]Civil Engineering Department, Benha Faculty of Engineering, Benha, Egypt.
[2]Civil Engineering Department, Delta University for science and technology, Gamasa, Egypt.

* Correspondence: aml.abdelaziz@bhit.bu.edu.eg

Citation:

A.Y.Kamal, A.M.Abou-Rayan, A.Shalabe, M.Samy, "Experimental investigation on the dynamic characteristics of a spar-type offshore wind turbine under irregular waves," Journal of Al-Azhar University Engineering Sector, vol. 18, pp. 830-849, 2023

Received: 07 July 2023

Accepted: 07 September 2023

DoI:10.21608/auej.2023.219019.1388

ABSTRACT

In the field of renewable energy, floating offshore wind turbines (FOWT) are currently a hot topic. Numerous numerical simulation programs have been developed to model the performance of FOWTs under wave condition in order to design and optimize them. To guarantee accurate results, numerical methods must, however, undergo model validation. Building a 1/300 scale model with a 3-leg catenary mooring allowed us to assess the OC3-Hywind spar platform's performance for this study.

To simulate real-world conditions, irregular wave states were generated in the Benha Faculty of Engineering laboratory where the model experiments were carried out. Our findings demonstrate that the surge, sway, heave, roll, pitch, and yaw responses of the model were accurately predicted by the Ansys-Aqwa numerical software. Moreover, the numerical software accurately predicted that the sway, roll, and yaw responses were significantly lower than the surge, heave, and pitch responses.

These results indicate that numerical simulation software, like Ansys-Aqwa, can provide precise predictions of the behavior of floating offshore wind turbines under wave conditions. The outcomes of our model testing can be used to verify the precision of these simulation programs and enhance their capacity for prediction.

KEYWORDS: Floating Offshore structures, Wind Turbines,OC3-Hywind spar platform, Quadratic Transfer Functions, Low wave-frequency.

تحت تأثير ذات العمود الواحد (السارية) دراسة معملية للخصائص الديناميكية لتوربينة الرياح البحرية الأمواج الغير المنتظمة

أحمد يوسف كمال 1 ، أشرف محمد أبوريان 1 ، أمل شلبي 1* ، محمد سامي 2

1قسم الهندسة المدنية ، كلية الهندسة جامعة بنها، بنها، مصر
2قسم الهندسة المدنية، كلية الهندسة جامعة الدلتا والتكنولوجيا، جمصا، مصر

***البريد الاليكتروني للباحث الرئيسي:** aml.abdelaziz@bhit.bu.edu.eg

الملخص العربي: -

في مجال الطاقة المتجددة ، تعد توربينات الرياح البحرية العائمة موضوعًا ساخنًا حاليًا. تم تطوير العديد من برامج المحاكاة العددية لنمذجة أداء توربينات الرياح البحرية العائمة تحت تأثير قوة الرياح والأمواج معا مجتمعة من أجل تصميمها وتحسينها. لضمان الحصول على نتائج دقيقة للتحليل النظري ، يجب أن تخضع الدراسة بتجارب معملية للتأكد من صحة النموذج . ولذلك قمنا بإنشاء نموذج بمقياس 300/1 موصول بثلاث سلاسل مثبتة، ولمحاكاة الظروف الطبيعية ، تم دراسة المنشأ تحت تأثير الموجات الغير المنتظمة في مختبر كلية الهندسة في بنها حيث تم إجراء عدة تجارب.

توضح النتائج التي توصلنا إليها أن استجابات النموذج التي تم الحصول عليها من قبل برنامج Ansys-Aqwa العددي تتوافق مع النتائج المعملية للنموذج وذلك في جميع درجات الحرية **الست للمنشأ** (ثلاث درجات حرية كإزاحات : الاتجاة الموازي للموجة ، الاتجاة العرضي على الاتجاة الموازي للموجة، الاتجاة العمودي على قطاع النموذج و ثلاث درجات حرية كحركة دورانية : حركة دورانية حول المحور في الاتجاة الموازي للموجة ، حركة دورانية حول المحور في الاتجاة العرضي على الاتجاة الموازي للموجة، حركة دورانية حول المحور في الاتجاة العمودي على قطاع النموذج). علاوة على ذلك ، توصلنا إلى استجابة المنشأ للحركة في الاتجاة العرضي على الاتجاة الموازي للموجة و حركة دورانية حول المحور في الاتجاة الموازي للموجة و الحركة الدورانية حول المحور في الاتجاة العمودي أقل من استجابة المنشأ للحركة في الاتجاة الموازي للموجة و الاتجاة العمودي و الدوران حول المحور في الاتجاة العرضي.

تشير هذه النتائج إلى أن برنامج المحاكاة الرقمية ، مثل Ansys-Aqwa ، يمكن أن يوفر تنبؤات دقيقة لسلوك توربينات الرياح البحرية العائمة تحت تأثير الأمواج. يمكن استخدام نتائج اختبار النموذج الخاص بنا للتحقق من دقة برامج المحاكاة هذه وتعزيز قدرتها على التنبؤ.

الكلمات المفتاحية : المنشآت البحرية العائمة، توربينات الرياح، توربينة الرياح ذات العمود الواحد (السارية)، وظائف التحويل التربيعية، التردد الموجي المنخفض.

1. INTRODUCTION

Considering current environmental issues like energy scarcity, pollution, and global warming, research on clean, new, and renewable energy is now essential. Numerous advancements in the field of renewable energy have been made over the last few years. There are several potential sources, including wind, tidal, solar, biological, and hydrodynamic; there has been a lot of research in this area recently. Technically and economically, wind energy seems to be the most reliable and valuable source of energy production. From wind farms that have been constructed over the past few years, electricity is produced by wind turbines.

Although offshore wind power is more effective, both onshore and offshore wind turbines produce wind energy. Due to the deep-sea environment, two foundation structures - a floating platform with a mooring system and a fixed foundation - have been suggested for offshore wind turbines. Depths of several hundred meters are typical in oceans where the wind source is significantly higher than the shore. A fixed foundation is more cost-effective for depths of 20 to 50 m.

Due to the scarcity of land, fixed offshore wind turbines have been installed in shallow waters recently. The tension leg platform (TLP) with different shapes (rectangular, triangular, and hexagonal) and the spar type system are the two most popular types of offshore supporting wind turbine structures for deep-sea locations with abundant wind. In our study, the spar type was looked at.

The spar floating platform can be modeled as a rigid body with six degrees of freedom (6-DOF). Heave, roll, and pitch motions make up the vertical degrees of freedom while surge, sway, and yaw motions make up the horizontal degrees of freedom.

Several studies on the dynamic behavior of spar-type FOWT have been conducted. For the purpose of evaluating numerical simulation methods for FOWTs, the current experiment serves as a benchmark that simulated a floating offshore wind turbine using spars (FOWT). The scaled OC3-Hywind FOWT model takes into consideration the pitch control mechanism, an ideal disc-plane anemometer arrangement technique increases the accuracy of wind field measurements. The rotor has a significant effect on yaw, and the trend and amplitude of structural rigid-body motion are dominated by aerodynamic and hydrodynamic loads, respectively. Load case testing is done in three different ways: wind-only, wave-only, and wind-wave concurrent load. Furthermore, the coupling effects of the rigid-body motions with multiple degrees of freedom (MDOF) of the structure are particularly evident. Although the flexible tower only slightly deforms, the resonance brought on by double frequency conjugation effects is substantial. Additionally, a sizable amplitude of tension can be generated in the flexible tower under wave-contained conditions [1].

It conducted an experimental campaign to analyze the dynamic behavior of offshore floating wind turbines (FOWT). The primary goal of this research is to provide measured data from experiments to demonstrate numerical software for nonlinear motion studies. According to the behavior, the snatching causes significant instantaneous stress on the mooring line tensions, and acceleration of the platform can cause the mooring line to break in the structure itself [2].

An experimental and numerical study on a 6MW spar-type FOWT system was conducted to investigate the nonlinear hydrodynamic response. The second-order Low wave-frequency (LF) wave loads are modeled in their study by applying two different strategies based on complete quadratic transfer functions (QTF) and Newman's approximation, respectively. Compared with Newman's method, the extended QTF method significantly improves the prediction of the LF response. Generally, the amplitude of the wave-frequency responses for surge and heave is greater than that of the LF responses. In contrast, the LF pitch motions are more significant than the equivalent WF contribution [3].

An investigation of the experimental and numerical response of a 6 MW spar-type FOWT constructed for a depth of 100 m. For the experiment, a scaled model was created with an aspect ratio of 65.3 and created a numerical model using the Fatigue, Aerodynamics, Structures, and Turbulence (FAST open-source platform). According to experimental and numerical investigations, they are dependable and consistent for the needed 6MW spar-type FOWT [4].

At the DHI tidal basin in Horsholm, Denmark, an experiment of an offshore spar buoy wind turbine's dynamic response was carried out under various wind and wave conditions. Uniform and unsteady waves with constant wind loads were forced to a scale model with a Froude ratio of 1:40. Before analysis, all experimental data were scaled to full scale using Froude scaling [5]. Additionally, a test for an OC3-Hywind spar buoy scale model in the University of Ulsan's Wide Tank was applied to look into the performance of the spar buoy. The model was constructed at a scale ratio of 1/128, and tests for diverse sea states, including the rotating rotor effect with the wind, were run. Following that, the outcomes were compared to numerical simulations. Significant oscillations and RAOs in both periodic and non-periodic waves are compared, and the results of these comparisons reveal similarities among model tests and the results of numerical analysis [6].

For the examination of the dynamic demeanor of a 1:50 scale model OC3 spar floating wind turbine, a concept was created for 200 m of water depth and irregular wind and wave forces were applied. To avoid some unfavorable effects of regulating wind turbine rotational speed seen in earlier studies, the rotor in the study could easily spin depending on the wind speed [7]. Additionally, the investigation the numerical and experimental dynamic responses of full-scale models of spar-type FOWTs with various variables of three design parameters (spar diameter, depth, and concrete ratio) under the wind, regular wave, and constant current loads carried out. ANSYS AQWA software was used to generate numerical analysis for various loading scenarios. The spar-type FOWT prototype was scaled up to 1:100 in comparison to the experimental model. The pitch motion results for the scale model were compared with numerical outcomes to confirm the numerical analysis's accuracy with experimental results. They demonstrated strong agreement in all loading scenarios. The ideal spar diameter was chosen after examining 15 models numerically and experimentally to achieve the lowest weight for the structure while maintaining structural stability. To increase the surge and pitch motions by decreasing the structure's depth [8].

The study of the dynamic behavior of a triangular, square, and pentagon TLP supporting a 5MW wind turbine exposed to multidirectional uniform and random waves that the environmental loads have been evaluated in accordance with the Egyptian Metrological Authority's data for the northern region of the Red Sea. The analysis was conducted using the ANSYS-AQWA, FAST, and MATLAB programs. Their findings improved our knowledge of dynamics and platform stability [9].

The investigations of the dynamic responses of triangular and square tension leg platforms under hydrodynamic forces using MATLAB software were carried out. Both studies were conducted to investigate the consequences of nonlinearities generated by hydrodynamic forces in the time domain, as well as the conjunction effect between surge, sway, heave, roll, pitch, and yaw degrees of freedom on the dynamic behavior of TLPs. The investigation only took into account unidirectional waves in the surge direction, and the responses of the two shapes were contrasted [10], [11].

To collect data on the coupled motions and loads between the identical wind turbine and the three floating supporting systems for the operations and maintenance, design, and survival of sea states, the authors tested three floating systems - a spar, a semisubmersible, and a tension-leg platform - each supporting a 1:50 scaled 5 MW wind turbine. to determine the benefits and drawbacks of the three floating platforms as well [12].

The authors investigated numerically the hydrodynamic properties of an OC3-Hywind spar-type wind turbine, and dynamic outcomes, and evaluated the response properties of motions and mooring loads in various sea states. In addition, they discussed the influence of wind and wave loads on the system. The FAST numerical modeling code is used for time domain calculations, and the FFT method is used for frequency analysis [13].

In an experimental and numerical study published in 2013, they looked at how the spar platform that supports the wind turbine responds to regular waves. Three phases of the experiments were performed: 1- Spar with a fixed wind turbine in a calm sea 2- Spar in calm seas with a rotating wind turbine 3. A rotating turbine-equipped spar in regular waves. A numerical analysis was performed using AQWA software. The analysis of numerical and experimental data shows that they are in good agreement [14]. Also, they numerically investigated the dynamic response of a spar-type hollow cylindrical floating supporting system attached by three catenary cables and forced by nonhomogeneous wave irritation. The upper part of the wind turbine was modeled as a lumped mass, with the nonhomogeneous wave flow generated using the Pierson-Moskowitz spectrum. The time-and-frequency responses of the spar platform and the tension of mooring cables are investigated in terms of total length and mooring cable connection position [15].

By changing the shape of the platforms, the authors tested three new spar platforms according to the OC3-Hywind Spar to support a 5-MW wind turbine. The models were built at the Ocean Engineering Tank with a 1/128 scale ratio and were forced by regular and irregular waves, as well a rotating rotor effect and mean wind speed. From measured data, RAOs and significant motions were computed and compared with those of the original OC3-Hywind spar, resulting in the three new platforms having better motion characteristics than the original OC3-Hywind spar [16].

Professors displayed the measured data of a half-scaled spar platform carrying a 100kW wind turbine to ensure the safety of a full-scale floater with a 2MW wind turbine be laid in the exact location as the half-scaled one once it is removed. Each of the six degrees of freedom and the tension force of the mooring lines was measured and tracked. Additionally, a powerful typhoon affected the half-scaled model. Still, it managed to survive even when the waves were higher than expected, so after the study, it was safe approval to install the full-sized spar platform wind turbine [17]. were concerned about using precast concrete parts at the bottom of the spar and joined them to the top steel part to show the effect on the economic condition of establishing the platform. The model was made with a 1/10 scale model of the prototype spar platform that held a 1kW wind turbine, installed, operated, and removed. Through this study, it was determined that the spar FOWT could work well enough for the prototype model to be used in the offshore area [18].

A scaled model of the spar platform by 1/34.5 scaled factor was tested at the Ocean Engineering Basin of National Maritime Research to make sure it was safe during a storm. The results showed that if one mooring line breaks during a storm, the floater is still safe because the other lines still hold it in place. Also, the mooring line is at its tightest when the wind, waves, and current come from a similar direction [19].

Previous researchers looked into the effects of long-crested waves on spar-platform response, whether under regular or irregular waves. Other authors investigated the spar-platform responses experimentally due to multidirectional waves that were categorized under short-crested waves. On classic and truss-spar platforms, they used unidirectional, bidirectional, and multidirectional waves. They discovered that short-crested waves, especially multidirectional waves, have less of an effect on the spar responses than lengthy-crest waves [20]. Also, they presented the findings of a numerical study for an offshore classic spar platform exposed to long-crest waves. The waves were simulated using the Morison equation and the Diffraction theory to demonstrate that either theory has an impact on the responses of the spar platform. The study found that when diffraction effects were not taken into account, the Morison force caused more surge and pitch motions [21].

To present the data of the nonlinear response of the square TLP structure a numerical investigation under various random waves was conducted. The Pierson-Moskowitz spectrum generated random waves that acted in the surge direction. Analyses were performed in both the time and frequency domains using MATLAB software [22]. Also, an experiment of a 1:87 scaled model of a classic petroleum spar platform was applied to confirm the predicted results. The study showed a similar and excellent agreement between predictions and test measurements [23].

This study compares numerical simulations to the outcomes of model scale experiments on the OC3 Hywind. In the offshore structures engineering lab of the Benha Faculty of Engineering, model tests were done with a 1/300 scale ratio to investigate the Spar wind turbine dynamic characteristics under irregular waves. Since it is very expensive to have a towing tank, the other objective of the experiment is to show that a small flume (with an ingenious system to reduce wave reflection) can gain a set of experimental data still suitable to calibrate the numerical model and give good results.

2. EXPERIMENTAL INVESTIGATION

2.1 Wave Tank Details And Wave Data

2.1.1 Wave tank

The experiments were conducted at the Benha Faculty of Engineering. The wave tank is 4.6 m long and 1.7 m wide, with a water depth of 1 m overall. The model is 1 meter from the wavemaker (Fig. 1, Fig. 2, Fig. 3). The wave tank body was made from iron sheets and the middle span of the tank from acrylic sheets to monitor the motion during the experiment.

Hinged-flap type wave maker is made with flat vertical plate hinged at the bottom and rotating around its axis by a centric disk motor so when driven with an oscillatory motion it partially rotates in a fore and aft arc. It is suited for physical modelling of deep-water waves, where the water is barely perturbed at the lower depth of the tank. The pitching motion about the submerged hinge is regarded as more inductive to quickly produce the correct water particle orbital profiles which also exhibit the required exponential diameter decay with depth. The wave maker can generate irregular waves. Since the tank length is not that long, we cannot make a beach at the end to soak up the wave energy, so an opening at the end of the tank was made to take wave overflow and then send it back through a pump behind the wave generator. With this tank modification, the impact of the back wave (wave reflection), which was affecting the responses, was minimized.

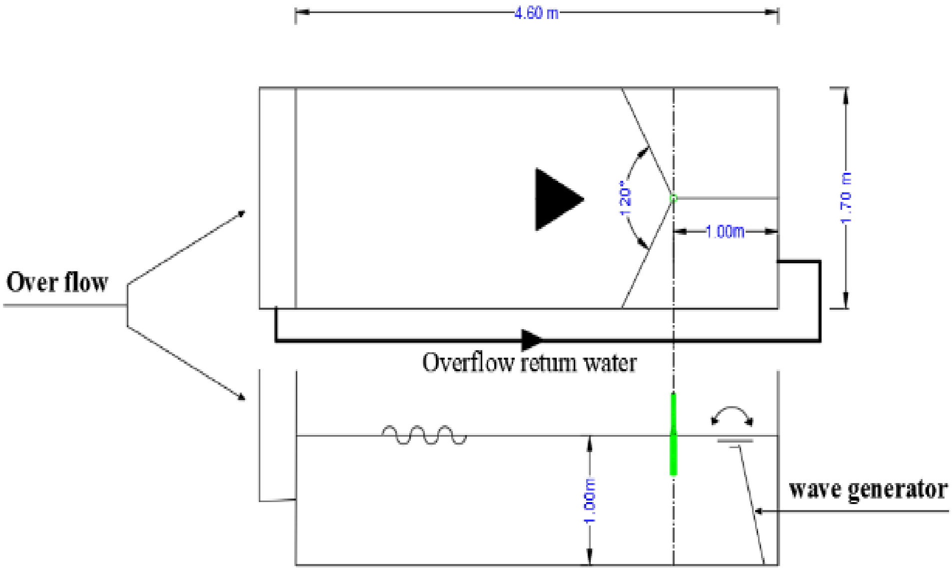

Fig. 1 :Wave basin layout

Fig. 2: Wave generator with its supporting system

Fig. 3: Wave basin and the overflow section (field photo)

2.1.2 Wave data

A liquid level sensor was used to measure the current wave data (Fig. 4, Fig. 5). The time history for the irregular wave is shown in Fig. 6. The average wave height is 2.1 cm, and the time period equals 3.2 sec. Fig. 7 shows the power spectrum density (PSD) chart for the wave excitation force, which shows that the excitation frequency of the generated wave is about 2 rad/sec.

Fig. 4: Liquid level sensor

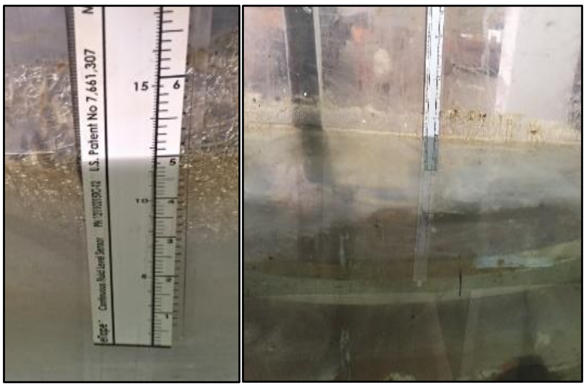

Fig. 5: Liquid level sensor during the experiment

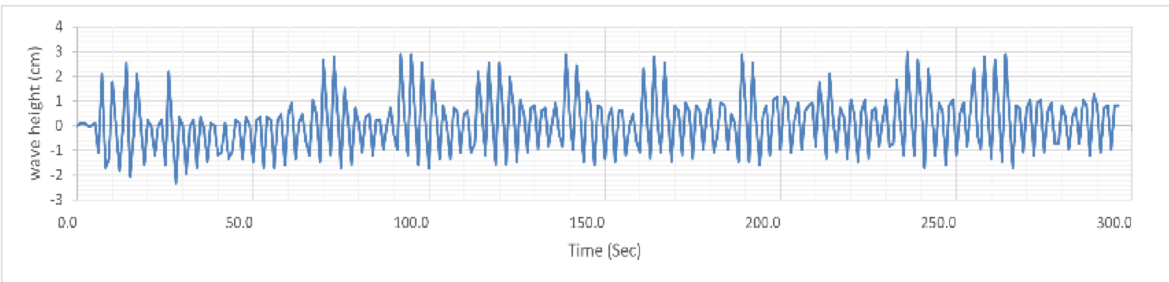

Fig. 6: Time history for wave excitation

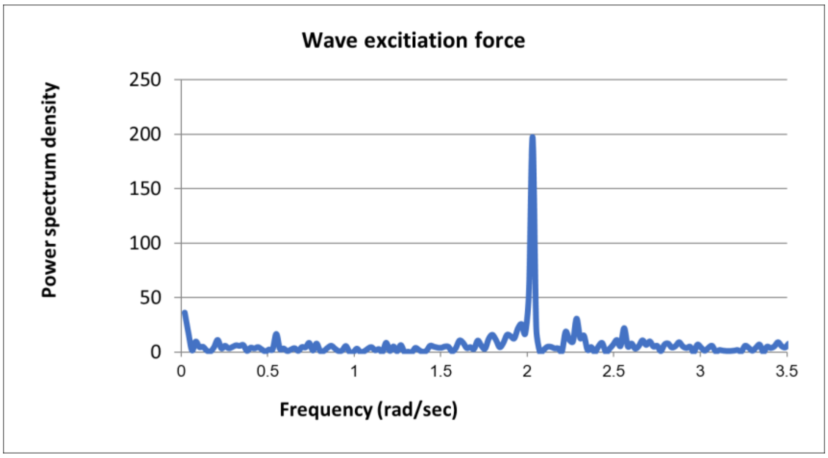

Fig. 7: Power spectrum density chart for the wave excitation force

2.2 Geometry Model And Mooring Line

2.2.1 Geometry model

The geometry model went through three stages: A- A 1:300 scaled model made of artilon with a ballast weight inside the model, but the model was sinking in the basin tank, B- then the scale decreased to 1:500, and the ballast weight was iron rings around the model, but it also sinks in the basin tank, C- final model is a scaled model of 1:300 scale factor for the prototype model OC3-Hywind spar buoy wind turbine structure (Fig. 8).

Table *1* summarizes the geometric properties of the OC3-Hywind SB (Spar Buoy) prototype model and experimental model. The model was created using the 3D printing method made of PLA plastic material at Benha Faculty of Engineering, composed of five parts: 1- Lower cylinder with 0.05 m diameter and a 0.36 m height, 2- Upper cylinder with a lower diameter equal to 0.05m, and an upper diameter of 0.02 m with a 0.14 m elevation, 3- Wind turbine tower with a height 0.24 m, 4- Hub diameter of 0.035m and a length of 0.09 m, 5- Rotor Blade of 0.21 m length. The ballast weight was made from lead material in the shape of a cylinder and was created by precasting.

Table 1: The SB-OC3 Hywind's geometric properties. Length Scale 1:300

SB OC3-Hywind	Full scale Dimension (m)	Scaled model Dimension (m)
SB diameter	15	0.05
Depth of floater base below SWL (total draft)	120	0.4
Tower height	88.50	0.295
Tower diameter	6	0.02
Hub diameter	3	0.01
Radius of fairleads	15	0.05
Depth of fairleads	70	0.23
Blade length	63	0.21

2.2.2 Mooring lines

The spar platform model is tethered to the ground by a set of three catenary lines through a circular connection, according to Fig. 9. The fairleads are positioned 0.025 m from the center of the platform and 0.23 m below the SWL. The nominal orientation of one of the lines is parallel to the positive X-axis (in the surge direction). At the platform, the two remaining lines are evenly separated by a 120° angle. The mooring line system's characteristics are displayed in Table 2.

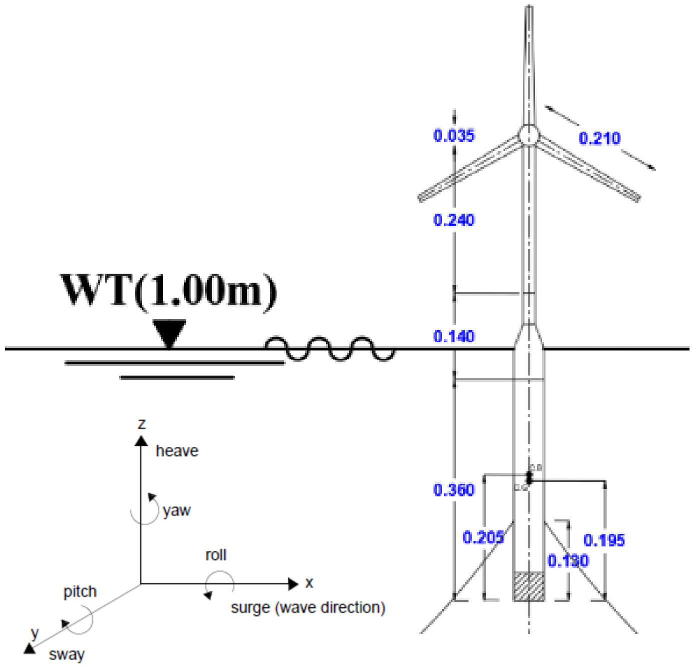

Fig. 8: A sketch for spar buoy wind turbine model

Fig. 9: Circular catenary connection

Table 2 :Mooring lines characteristics

Description	Unit	Full scale	Scaled model
Mooring line in Diameter	m	0.09	0.000295
Unstretched length	m	902.2	3.01
Equivalent mass density	Kg/m	77.7706	0.000863
Mooring point (from bottom)	m	50	0.13
Number of mooring lines	-	3	3

2.3 Motion Monitor Sensor

A system of electronic sensors was used to measure the responses to the spar model. The system consists of an Esp32- Arduino, imu (GY85), and a power bank as a power supply. The Esp32-Arduino is a family of inexpensive, low-power systems on a chip with dual-mode Bluetooth and integrated Wi-Fi that is used to receive data from the imu (gy85) sensor and send it to the laptop via Wi-Fi so that the experiment's results (real-time recording of data) operation can be seen on the screen. The imu (gy85) is a 9DOF sensor module based on an accelerometer, gyroscope, and magnetometer used to measure the spar model's acceleration and rotation during the experiment. It settled inside the spar model near the center of mass and connected to the Esp32-Arduino. Fig. 10 displays a schematic diagram of the electronic sensor system and the process of measuring the responses during the experiment.

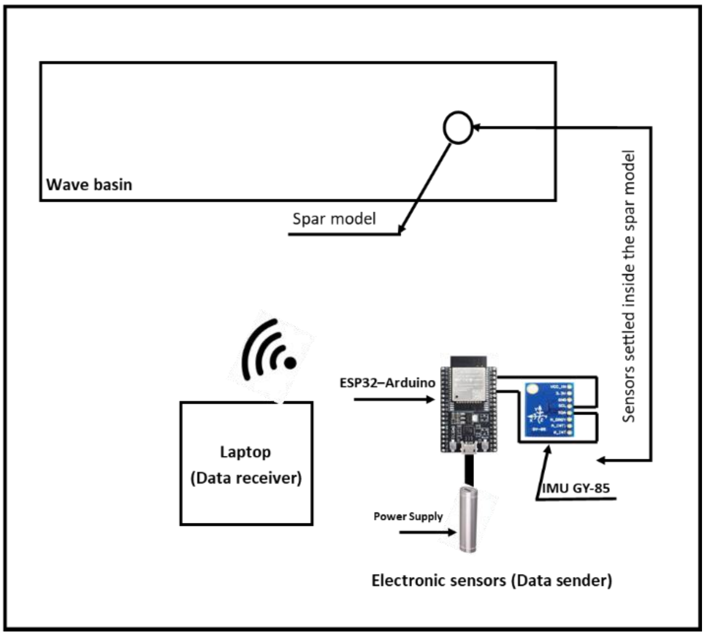

Fig. 10: Schematic diagram for the experiment

2.4 Experimental Test

As shown in Fig. 11, the spar model was positioned in the middle of the tank's width, one meter away from the wave generator. The wave direction was considered to be acting on the model surge direction. The experiment procedure was repeated several times to obtain stable results and accurately study the spar model's dynamic responses.

Fig. 11: Spar model during the experiment

3. NUMERICAL INVESTIGATION

The numerical model was produced for the OC3-Hywind spar offshore structure using ANSYS-AQWA (version 15.0) Fig. 12. The numerical model was assigned as a thin body geometry its properties were calculated using SOLIDWORKS software, where

Table *3* shows the model properties. the catenaries were assigned as a Non-Linear catenary and their properties are shown in Table 2.

The numerical model simulated the Spar wind turbine's response to the same environmental circumstances as the experiment. Many numerical models were tested and compared with experimental ones. But the waves are very far from the experimental ones. This was due to the fact that the irregular waves used in the Ansys-Aqwa were either Jonswap (Hs), Jonswap (Alpha), Pierson-Moskowitz, or Gaussian; these waves had a more efficient spectrum than the real one. So, the actual wave data (experimental) was digitized and used as an input for the excitation wave in the numerical model, which means that the numerical and experimental models have the same excitation. The numerical model excitation (wave parameters) was calculated by multiplying the real wave data from the experiment by the Froude scaling ratio.

Properties	Unit	Full scale
Mass	Kg	41671093.93239
Center of gravity	m	81.52
Second moment of inertia Ixx	$Kg.m^2$	429669321997.934
Second moment of inertia Iyy	$Kg.m^2$	429669321997.934
Second moment of inertia Izz	$Kg.m^2$	1672003710.34637

Table 3: Numerical model properties

Properties	Unit	Full scale
Mass	Kg	41671093.93239
Center of gravity	m	81.52
Second moment of inertia Ixx	$Kg.m^2$	429669321997.934
Second moment of inertia Iyy	$Kg.m^2$	429669321997.934
Second moment of inertia Izz	$Kg.m^2$	1672003710.34637

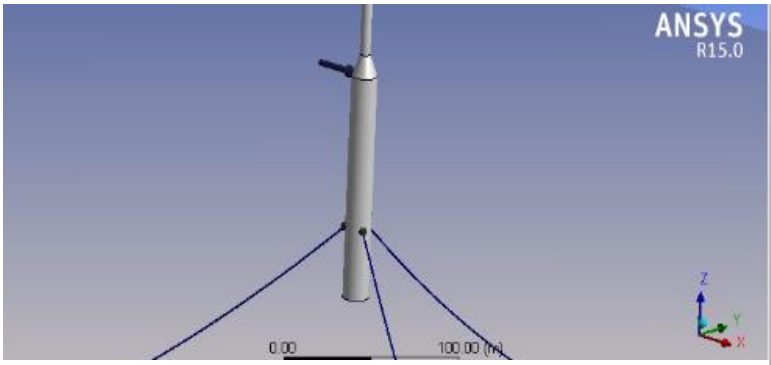

Fig. 12: A screenshot for numerical analysis of the spar structure using Ansys-Aqwa

4. RESULTS AND DISCUSSION

A Finite Element model with a numerical method was created to compare its responses with those discovered through the experiment. Data has been collected for the 6 DOF for a long time. While there are numerous data points from the experiment and numerical model, only the most important ones are shown.

4.1 Surge Response

Fig. 13, displays a sample of the time history for the numerical (Ansys-Aqwa) and experimental results. The surge motion collected from the experiment appears to be in excellent agreement with numerical ones. As seen in Fig. 14, the motion (trajectory) is a one-periodic motion with local chaos. This local chaos could be attributed to the back wave effect and the irregularity of the wave. The power spectrum density supports this in Fig. 15. The surge frequency is about 4.4 rad/sec for the experimental results shown in the power spectrum density chart Fig. 15. It's important to note that the experimental data were scaled using the Froud scaling factor.

As seen from Fig. 13, notches appeared in the time history due to the back-wave accumulation, which interfered with the generated wave causing a disturbing motion in the response time history.

Also, the difference in the initial conditions, especially for the test, is responsible for the phase shift between the experiment and the numerical model results. It is clear from the figure that surge responses have a higher energy content than other responses because the wave is in the surge direction of the model.

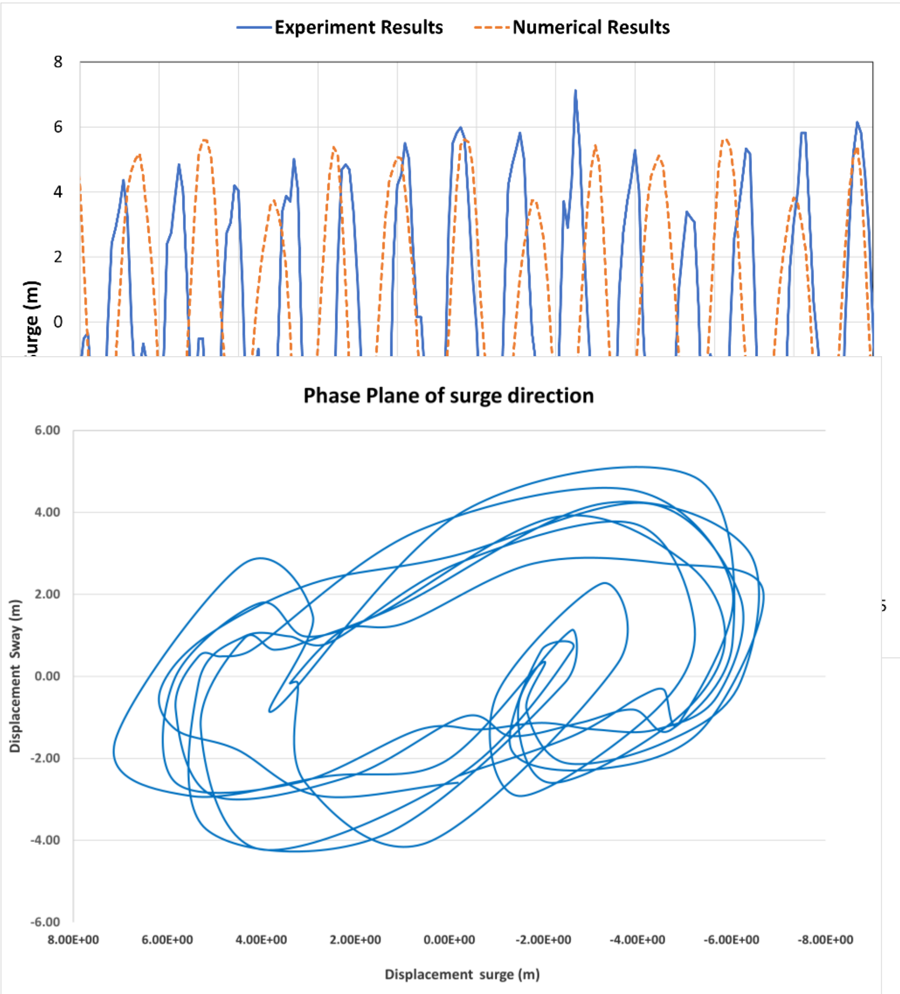

Fig. 14: Phase plane for surge motion

4.2 Sway Response

A very small sway response was noticed due to the irregular wave excitation, as seen in Fig. 16 since the wave is in the surge direction. The sway response frequency is equal to 4.5 rad/sec, shown in Fig. 17.

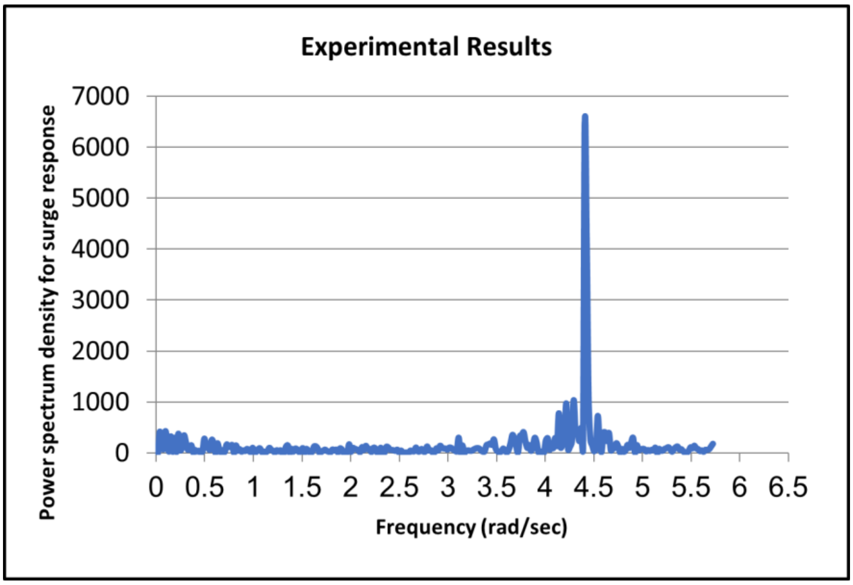

Fig. 15: Power spectrum density chart for surge response

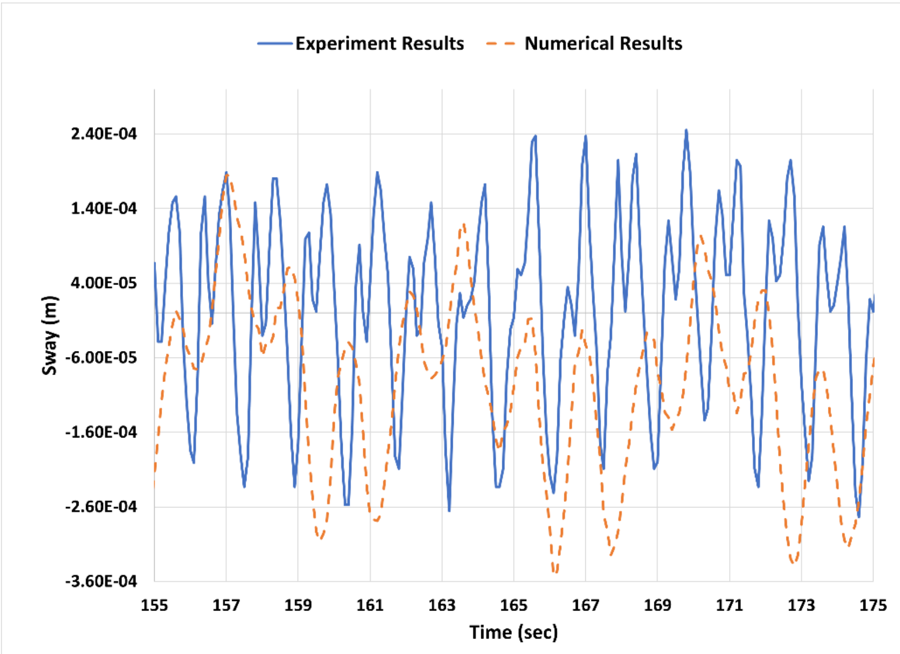

Fig. 16: Time history of sway response

4.3 Heave Response

Fig. 18 and Fig. 19 represent the time history of the numerical and experimental outcomes for the heave responses and the PSD chart, respectively. The results indicate that the numerical and experimental results agree well. Also, from the power spectrum density chart, the frequency was about 4.49 rad/sec.

Once more, the difference in the initial condition is what causes the phase shift between the numerical and experimental results. Also, the notches in experimental data are due to the back wave effect. From Fig. 19, it is clear that the heave motion has a smaller energy content than the one in surge response, which is good for the stability of the floating structure.

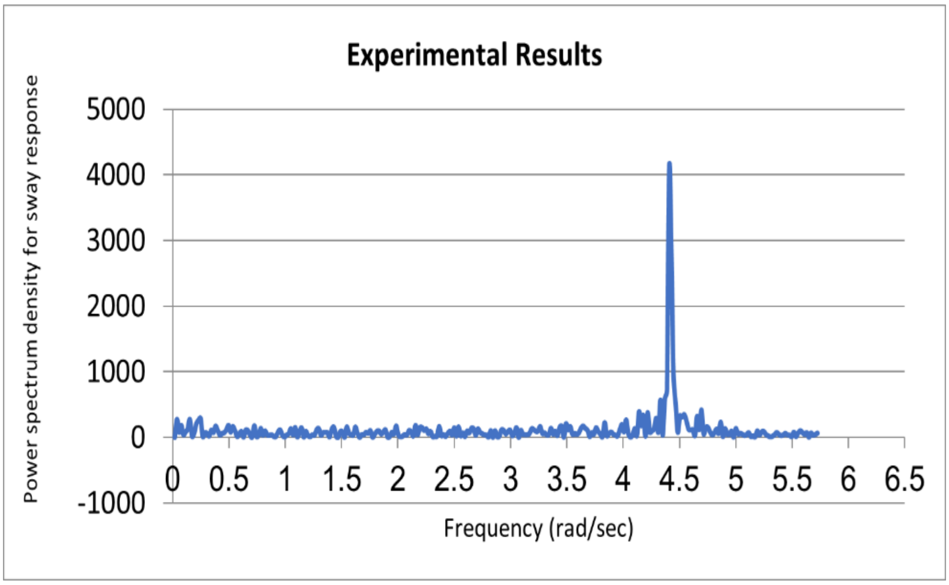

Fig. 17: Power spectrum density chart for sway response

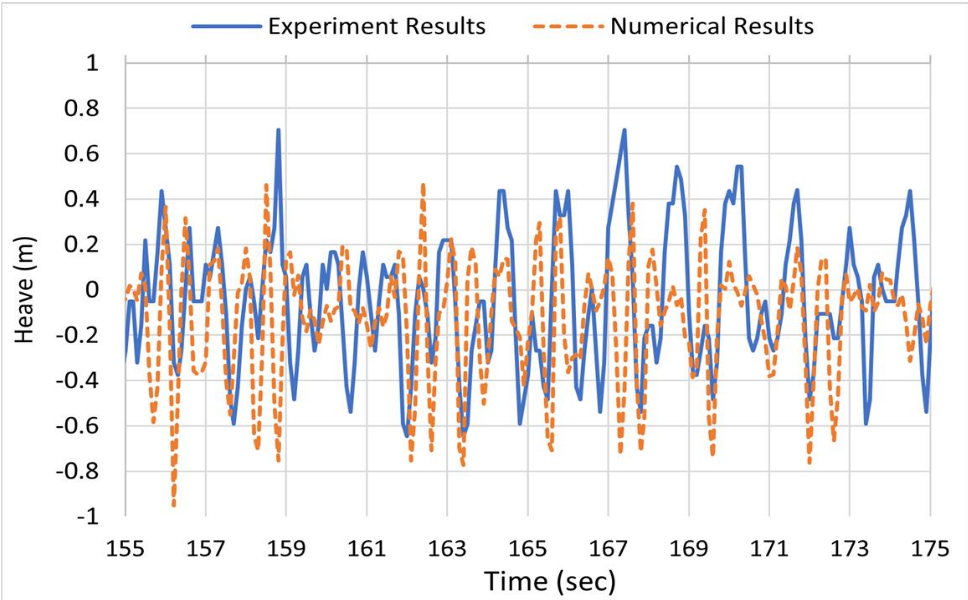

Fig. 18: Time history of heave response

4.4 Roll And Yaw Responses

There are very slight responses in the roll and yaw directions. Still, the numerical and experimental data for the spar model also agree well, as can be seen in Fig. 20 and Fig. 21, which indicates that the structure is stable and does not rotate about its vertical axis nor the about wave direction axis. The frequency response for the roll and yaw responses is 4.5 rad/sec, as shown in PSD charts Fig. 22 and Fig. 23. Again, the notches and the phase shift are due to reasons stated before in the surge response.

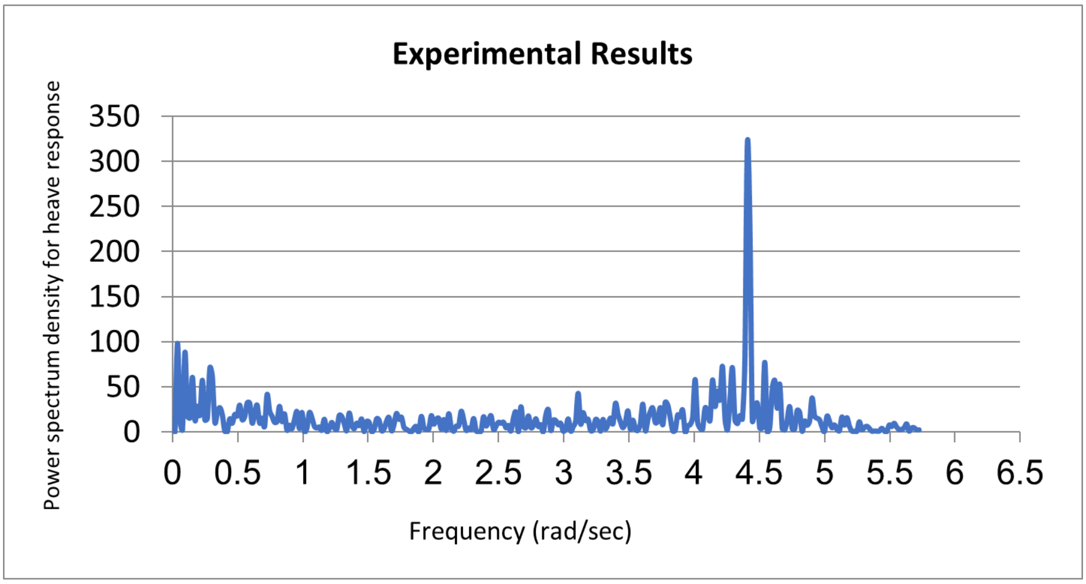

Fig. 19: Power spectrum density chart for heave response

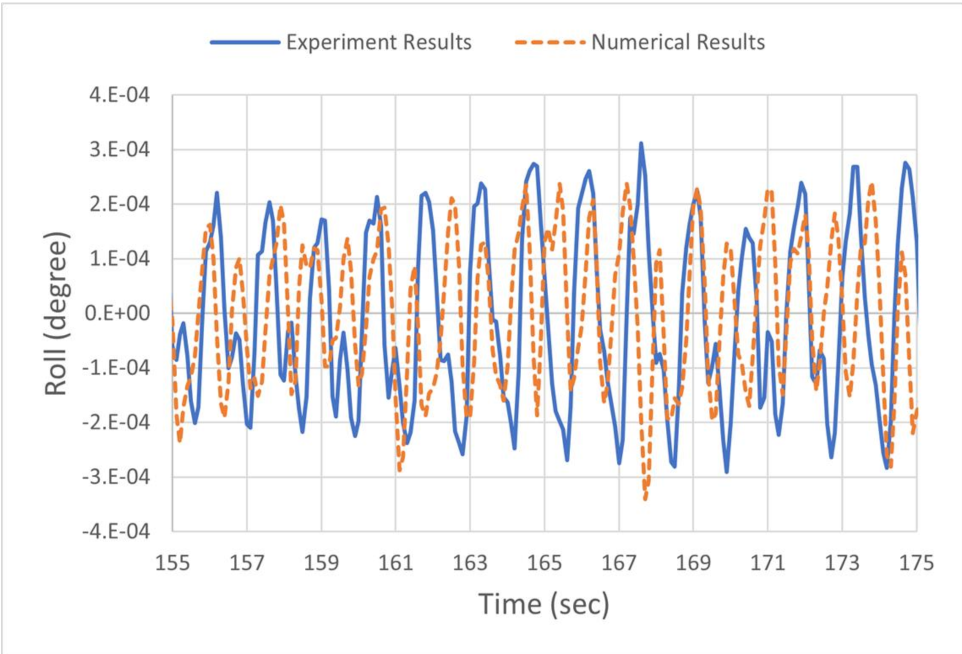

Fig. 20: Time history of roll response

4.5 Pitch Response

According to the data, Fig. 24 shows the numerical and experimental results for the pitch responses to motion. These results are in good agreement. Fig. 25 shows the PSD for pitch responses, where the frequency was found to be 4.49 rad/sec.

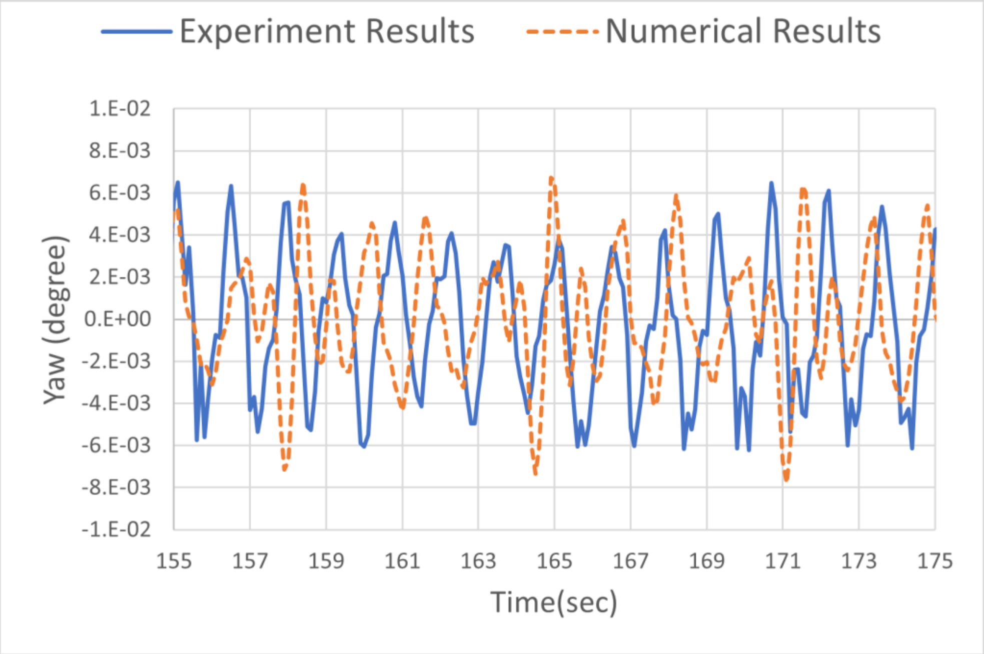

Fig. 21: Time history of yaw response

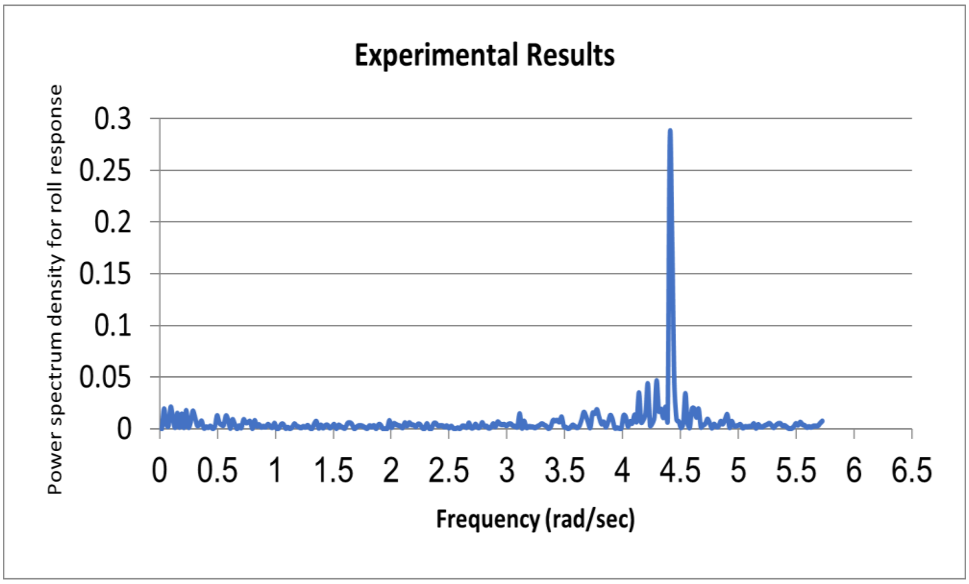

Fig. 22: Power spectrum density chart for roll response

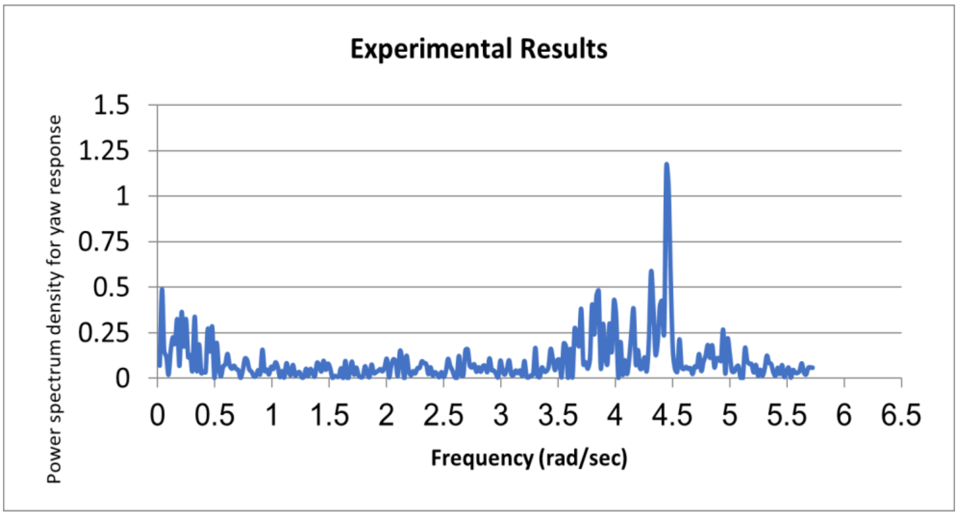

Fig. 23: Power spectrum density chart for yaw response

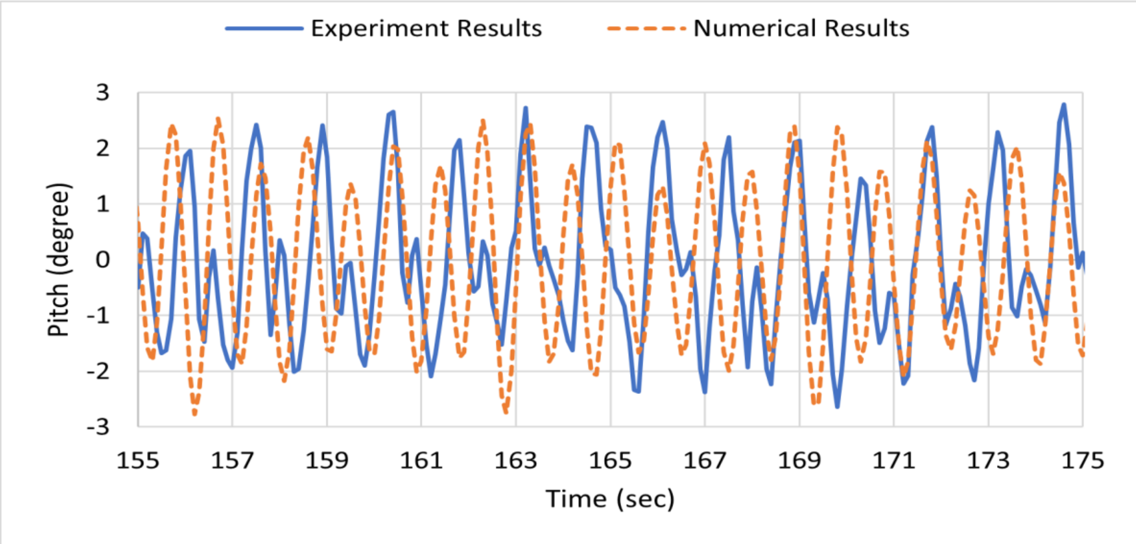

Fig. 24: Time history of pitch response

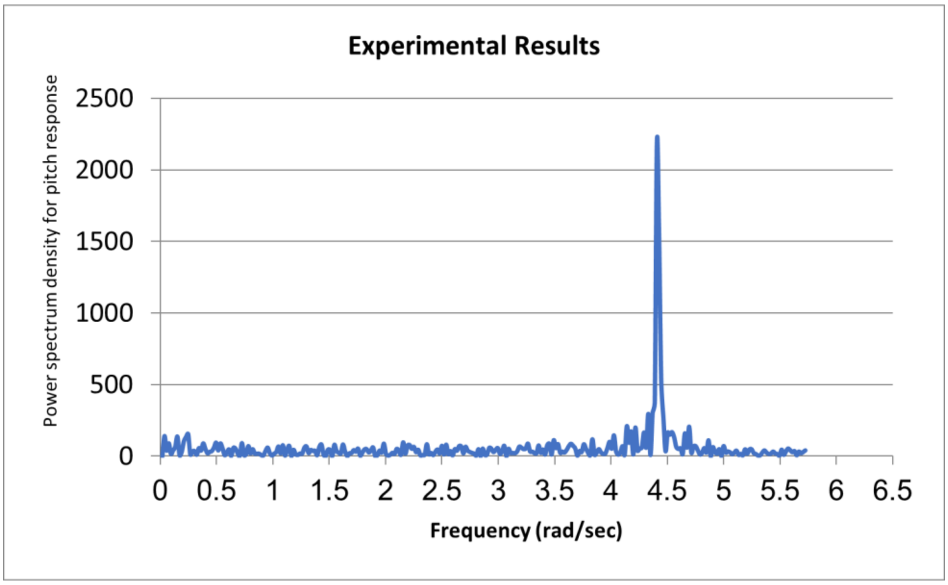

Fig. 25: Power spectrum density chart for pitch response

5. SUMMARY AND CONCLUSIONS

In this paper, a 1:300 spar OC3 model was investigated experimentally at the Benha faculty of engineering lab and numerically using Ansys-Aqwa software under irregular waves. The conclusions listed below can be drawn based on the results presented in this manuscript:

1) The numerical model and the experimental model agree very well.
2) The model responds well in the pitch and surge directions.
3) In comparison to the surge, pitch, and heave responses, the sway, roll, and yaw responses are very small. As seen that surge motion reached between 6m to 8m, pitch motion reached between 2° to 3° and heave motion was between 0.6m to 0.8m, on the other hand, sway motion reached a maximum of 2.4e-4 also, roll, and yaw motions respectively was maximum 3e-4° and 6e-3°.
4) The experiment model response results are somehow disturbed due to the back wave effect and the small size of the basin.
5) From all previous results (experimental), it is clear that the system is well away from the resonance state (excitation frequency is about 2.0 rad/sec, and all response frequencies are about 4.5 rad/sec).

CONFLICT OF INTEREST

The authors have no financial interest to declare in relation to the content of this article.

REFERENCES

[1]. J. Chen, Z. Liu, Y. Song, Y. Peng, & J. Li., (2022), "Experimental study on dynamic responses of a spar-type floating offshore wind turbine". Renewable Energy, 196, 560–578. https://doi.org/10.1016/j.renene.2022.06.149.

[2].X. Xu, & S. Day., (2021), "Experimental investigation on dynamic responses of a spar-type offshore floating wind turbine and its mooring system behavior". Ocean Engineering, 236, 109488. https://doi.org/10.1016/j.oceaneng.2021.109488.

[3].J. Yang, Y.-P. He, Y.-S. Zhao, Y.-L. Shao, & Z.-L. Han., (2021), "Experimental and numerical studies on the low-frequency responses of a spar-type floating offshore wind turbine". Ocean Engineering, 222, 108571. https://doi.org/10.1016/j.oceaneng.2021.108571.

[4].L. Meng, Y.-ping. He, Y.-sheng Zhao, J. Yang, H. Yang, Z.-long. Han, L. Yu, W.-gang. Mao, & W.-kang. Du., (2020), "Dynamic response of 6MW SPAR type floating offshore wind turbine by experiment and numerical analyses". China Ocean Engineering, 34(5), 608–620. https://doi.org/10.1007/s13344-020-0055-z.

[5].G. R. Tomasicchio, F. D'Alessandro, A. M. Avossa, L. Riefolo, E. Musci, F. Ricciardelli, & D. Vicinanza., (2018), "Experimental modelling of the dynamic behaviour of a spar buoy wind turbine". Renewable Energy, 127, 412–432. https://doi.org/10.1016/j.renene.2018.04.061.

[6].H.-J. Ahn, & H. Shin., (2019), "Model test and numerical simulation of OC3 spar type floating offshore wind turbine". International Journal of Naval Architecture and Ocean Engineering, 11(1), 1–10. https://doi.org/10.1016/j.ijnaoe.2017.09.010.

[7].F. Duan, Z. Hu & J. M. Niedzwecki., (2016), "Model test investigation of a spar floating wind turbine". Marine Structures, 49, 76–96. https://doi.org/10.1016/j.marstruc.2016.05.011.

[8].S. Rahmdel, B. Wang, C. Han, K. Kim, & S. Park., (2015), "A parametric study of spar-type floating offshore wind turbines (fowts) by numerical and experimental investigations". Ships and Offshore Structures, 11(8), 818–832. https://doi.org/10.1080/17445302.2015.1073865.
[9].A. M. Abou-Rayan, N. N. Khalil, & M. S. Afify., (2016), "Dynamic behavior of TLP's supporting 5-MW wind turbines under multi-directional waves". Ocean Systems Engineering, 6(2), 203–216. https://doi.org/10.12989/ose.2016.6.2.203.
[10].A. M. Abou-Rayan, A. A. Seleemah, & A. R. El-Gamal., (2012), "Response of square tension leg platforms to hydrodynamic forces". Ocean Systems Engineering, 2(2), 115–135. https://doi.org/10.12989/ose.2012.2.2.115.
[11].A.M. Abou-Rayan., (2014), "Dynamic Characteristics of Offshore Tension Leg Platforms Under Hydrodynamic Forces", International Journal of Civil Engineering (IJCE) Vol. 3, Issue 1, 7-16
[12].B. J. Koo, A. J. Goupee, R. W. Kimball, & K. F. Lambrakos., (2014), "Model tests for a floating wind turbine on three different floaters". Journal of Offshore Mechanics and Arctic Engineering, 136(2). https://doi.org/10.1115/1.4024711.
[13].Y. Ma, Z.-qiang. Hu, & L.-fei. Xiao., (2014), "Wind-wave induced dynamic response analysis for motions and mooring loads of a spar-type offshore floating wind turbine". Journal of Hydrodynamics, 26(6), 865–874. https://doi.org/10.1016/s1001-6058(14)60095-0.
[14].S. Nallayarasu, & S. Saravanapriya., (2013), "Experimental and numerical investigation on hydrodynamic response of spar with wind turbine under regular waves". The International Journal of Ocean and Climate Systems, 4(4), 239–260. https://doi.org/10.1260/1759-3131.4.4.239.
[15].S. H. Jeon, Y. U. Cho, M. W. Seo, J. R. Cho, & W. B. Jeong., (2013), "Dynamic response of floating substructure of spar-type offshore wind turbine with catenary mooring cables". Ocean Engineering, 72, 356–364. https://doi.org/10.1016/j.oceaneng.2013.07.017.
[16].H. Shin, P. T. Dam, K. J. Jung, J. Song, C. Rim, & T. Chung., (2013), "Model test of new floating offshore wind turbine platforms". International Journal of Naval Architecture and Ocean Engineering, 5(2), 199–209. https://doi.org/10.2478/ijnaoe-2013-0127.
[17].S. Ishida, K. Kokubun, T. Nimura, T. Utsunomiya, I. Sato, & S. Yoshida., (2013), "At-sea experiment of a hybrid spar type offshore wind turbine". Ocean Renewable Energy, Volume 8. https://doi.org/10.1115/omae2013-10655.
[18].T. Utsunomiya, H. Matsukuma, S. Minoura, K. Ko, H. Hamamura, O. Kobayashi, I. Sato, Y. Nomoto, & K. Yasui., (2013), "At sea experiment of a hybrid spar for floating offshore wind turbine using 1/10-scale model". Journal of Offshore Mechanics and Arctic Engineering, 135(3). https://doi.org/10.1115/1.4024148.
[19].K. Kokubun, S. Ishida, T. Nimura, T. Chujo, S. Yoshida, & T. Utsunomiya., (2012), "Model experiment of a SPAR type offshore wind turbine in storm condition". Ocean Space Utilization; Ocean Renewable Energy Volume 7. https://doi.org/10.1115/omae2012-83993.
[20].V. J. Kurian, C. Y. Ng, & M. S. Liew., (2012), "Experimental investigation on dynamic responses of spar platforms subjected to multi-directional waves". 2012 IEEE Business, Engineering & Industrial Applications Colloquium (BEIAC). https://doi.org/10.1109/beiac.2012.6226094
[21].V. J. Kurian, C. Y. Ng, & M. S. Liew., (2012), "Dynamic responses of classic spar platforms subjected to long crested waves: Morison equation vs. diffraction theory". 2012 International Conference on Statistics in Science, Business and Engineering (ICSSBE). https://doi.org/10.1109/icssbe.2012.6396620.
[22].M. Ashraf. Abou-Rayan, and S. Osama. Hussein., (2015),"Influence of wave approach angle on square TLP's behavior in random sea", the 2015 world congress, ASEM15, Incheon, Korea, August 25-29.
[23].A. Steen, M. H. Kim, & M. Irani., (2004), "Prediction of spar responses: Model tests vs. analysis". Offshore Technology Conference. https://doi.org/10.4043/16583-ms.